



# Effect of extra-framework Al formed by successive steaming and acid leaching of zeolite MCM-22 on its structure and catalytic performance

R.M. Mihályi<sup>a</sup>, M. Kollár<sup>a</sup>, P. Király<sup>b</sup>, Z. Karoly<sup>c</sup>, V. Mavrodinova<sup>d,\*</sup>

<sup>a</sup> Institute of Nanochemistry and Catalysis, Chemical Research Center, Hungarian Academy of Sciences, Pusztaszeri út 59-67, Budapest 1025, Hungary

<sup>b</sup> Institute of Structural Chemistry, Chemical Research Center, Hungarian Academy of Sciences, Pusztaszeri út 59-67, Budapest 1025, Hungary

<sup>c</sup> Institute of Materials and Environmental Chemistry, Chemical Research Center, Hungarian Academy of Sciences, Pusztaszeri út 59-67, Budapest 1025, Hungary

<sup>d</sup> Institute of Organic Chemistry with Centre of Phytochemistry, Bulgarian Academy of Sciences, Acad. G. Bonchev str., bl. 9, 1113 Sofia, Bulgaria

## ARTICLE INFO

### Article history:

Received 21 October 2011

Received in revised form 1 December 2011

Accepted 16 December 2011

Available online 27 December 2011

### Keywords:

MCM-22 zeolite

Steam-acid dealumination

Extra-framework Al

*m*-Xylene conversion

Coke formation

## ABSTRACT

Dealuminated MCM-22 samples have been prepared by a two-step dealumination procedure. Detailed assessment of the properties of the materials obtained at each one of the successive stages, i.e. steaming (at 500 °C, 700 °C and 800 °C) and acid reflux (HCl and oxalic), has been made by XRD, N<sub>2</sub> adsorption–desorption, *m*-xylene adsorption, <sup>27</sup>Al MAS NMR and FT-IR of pyridine adsorption. It was found that steaming generates extra-framework aluminum (EFAl) species and the majority of them cannot be extracted by the consecutive acid leaching. These extra-lattice entities block the zeolite micropores which makes the remaining Brønsted acid sites isolated and inefficient. It is shown that the presence of such species vastly affects the catalytic performance of zeolite MCM-22 in the reaction of *m*-xylene conversion. The consequences are reduced adsorption capacity and catalytic activity, modified reaction products distribution, enhanced *p*-xylene selectivity, as well as altered mode of coke formation and composition of the coke precursors.

© 2011 Elsevier B.V. All rights reserved.

## 1. Introduction

Dealumination of zeolite has been studied for several decades but recently the interest towards this modification method has been renewed as one of the several top down approaches for mesopore formation and creation of enhanced Brønsted acid sites, both crucial factors in determining the activity and selectivity in the transformations of aromatic hydrocarbons on zeolite catalysts [1]. Among the typical examples for such procedure, giving rise to a very significant catalyst improvement, are the well-known ultra-stable Y (USY) family materials featuring mesopores [2] which are obtained by dealumination via steam treatments and are being widely used in the petrochemical industry. The effectiveness of dealumination by steaming and/or acid leaching depends on both the severity of the procedure and the zeolite structure. During this treatment extra-framework aluminum species (EFAl) are generally formed, which could be removed from the lattice, and secondary mesoporosity might be created [3]. The non-framework aluminum generated by hydrothermal treatment can be easily extracted by the subsequent acid leaching but only in case of three-dimensional, large-pore zeolites [4,5]. Dealumination of more siliceous zeolites,

such as ZSM-5 or other structures induces rather limited mesoporosity [6–8].

The literature survey reveals that oxalic acid extracts the aluminum expelled upon previous hydrothermal treatment only from large-pore but not from medium-pore zeolites because of diffusion limitations [9,10]. Mordenite is suggested to imply diffusion problems too in removing, by mineral acid treatment, the EFAl from its one-dimensional pore structure [11]. It is observed by Fernandes et al. [12] that not only in mordenite but also for zeolite beta, steam dealumination generates highly polymerized EFAl which can be partially removed by the subsequent acid leaching.

The particular structure of the zeolite MCM-22 holds out interesting opportunities for studying the process of dealumination and the consequences of this procedure for its catalytic performance [13]. This zeolite is composed of two channel systems, both of them accessible through narrow 10-MR windows [14]. The material contains at least five crystallographically non-equivalent T-sites and they are affected to different extents by the mineral acid dealumination [13]. Partial dealumination takes place still during the calcination of this lamellar structure [15]. Dealumination is more severe on heating in air than in vacuum or N<sub>2</sub>, and may occur even during grinding in a mortar [16].

Studies on hydrothermally dealuminated MCM-22 zeolites show that aluminum released from the lattice mainly stays in the internal pore systems and then condenses into polymeric aluminum species, which causes a decrease in the accessibility of the

\* Corresponding author. Tel.: +359 2 979 3961; fax: +359 2 8700225.

E-mail addresses: [vmavrodinova@orgchm.bas.bg](mailto:vmavrodinova@orgchm.bas.bg), [vesselinamavrodinova@yahoo.com](mailto:vesselinamavrodinova@yahoo.com) (V. Mavrodinova).

acid sites to reactant molecules [17–20] and makes its channel system tighter by deposition of octahedral aluminum debris in the pores [21,22].

Dealumination of MCM-22 only with mineral acids seems to be a complex process. According to Matias et al. [13], first a rapid dissolution of the EF aluminum hydroxylated species formed upon calcination takes place, followed by slower extraction of the lattice Al. Higher diffusion limitations induced by the remaining EFAl species, not removed from the inner pore system of MCM-22 zeolite, are proposed by these authors. It appears that, for the confined channel system of MCM-22, the ability for dealumination strongly depends on the size of the applied acid molecule. Xia et al. [23] found differences in the effectiveness in dealumination using citric or oxalic acid, in favor of the ability of the smaller oxalic anion to enter easier into the zeolite channels. According to Unverricht et al. [24] the treatment of MCM-22 with 14.5 nHNO<sub>3</sub> even for 30 h does not result in a significant dealumination. The possible reason is the high stability of this zeolite against acid attack. Oxalic acid reflux of H-MCM-22 causes partial removal of the external acid sites according to Ren et al. [25].

The peculiarities of the successive steam-acid dealumination of zeolite MCM-22 are not investigated in details. Neither the change in the concentration and nature of the EFAl species formed and remained at each stage of this procedure, nor their role in the catalytic performance, are clarified sufficiently. There are only few studies on subsequent steam-acid dealuminated MCM-22 zeolite [26–29]. With the exception of the contribution of Park et al. [26] who do not find any promotion effect of the steam-acid dealuminated MCM-22 for the reaction of methylation of 2-methylnaphthalene, other researchers [27–29] ascertain that the activity of the as-modified catalysts in the reactions of alkylaromatic transformations (toluene and ethylbenzene) is reduced but the selectivity towards the *p*-substituted aromatics is enhanced. Presence of EFAl species is presumed only by Wu et al. [29] but the consequences of this presence are neglected. Analysis of the content and composition of these entities has not been made and their effect on the catalytic performance in the examined reactions has not been mentioned in any of the above contributions [27,28] but the one of Wu et al. [29]. The conclusion of the only authors that study steam-acid dealuminated MCM-22 in the reactions of toluene and ethylbenzene conversion is that aluminum is hardly removable from this zeolite type, but the formed EFAl species are highly dispersed within the crystallites, without blocking the micropores and without affecting at all the catalytic performance [27,29].

The last statement remains questionable considering the very recent studies on acid leached [13,23] or only hydrothermally treated [21–23] MCM-22 zeolites. The thorough <sup>27</sup>Al MAS NMR investigations implemented there evidence the effect of the presence, nature and variations of the extra-framework aluminum detected after dealumination [21–23] on the reaction selectivity in different catalytic transformations [13,23].

In the present work two-step dealumination procedure has been performed. At the first step the samples were hydrothermally treated, and then oxalic or hydrochloric acid reflux was applied in order to extract the EFAl species and to generate, eventually, a secondary mesopore channel system. The structural changes and the alteration in the catalytic performance occurred at each dealumination step have been thoroughly investigated. Our objective was to prove whether any mesoporosity can be generated at all by successive steam-acid dealumination of MCM-22 and to assess the effect of the EFAl generated within the pore structure of these materials on their catalytic activity and selectivity to isomerization and disproportionation of *m*-xylene as well as on the mode of coke formation.

## 2. Experimental

### 2.1. Catalysts preparation

The MCM-22 precursor was prepared by hydrothermal synthesis applying rotating industrial autoclave (~1 m<sup>3</sup>) according to the procedure described in Ref. [30]. The composition of the synthesis gel was SiO<sub>2</sub>:0.036Al<sub>2</sub>O<sub>3</sub>:0.024Na<sub>2</sub>O:0.265Na<sub>2</sub>SO<sub>4</sub>:0.517 hexamethylenimine:42.6H<sub>2</sub>O. The crystallization temperature and time were 418 K and 10 days respectively, and sample with Si/Al molar ratio of 16 was obtained. After washing with distilled water and drying at 343 K, the preparation was calcined in air (programmed heating, 1.5 K/min up to 823 K for 3 h) in order to remove the template. Twofold ion exchange with 1 M NH<sub>4</sub>NO<sub>3</sub> solution was applied for the preparation of the ammonium form. The H-form of the sample was obtained by *in situ* decomposition of the NH<sub>4</sub><sup>+</sup>-forms in N<sub>2</sub> at 823 K and is indicated as MCM-22 (Table 1). The dealumination procedure was carried out by steam treatment at 773 K (500 °C), 973 K (700 °C) or 1073 K (800 °C) (samples designated as D500, D700 and D800) followed by either 2 M HCl (D700/HCl and D800/HCl) or 0.5 M oxalic (D500/Ox and D700/Ox) acid reflux at 373 K (Table 1).

### 2.2. Catalysts characterization

The structure and crystallinity of the samples were verified by a Philips PW 1810 powder diffractometer. Adsorption isotherms were determined by N<sub>2</sub> sorption at 77 K using a Quantachrome NOVA Automated Gas Sorption instrument. The specific surface area was calculated from the N<sub>2</sub> adsorption capacity by the multiple BET method. The micropore volumes were estimated from the alpha-s plots. The acidity of the materials was determined by FT-IR (Nicolet Impact Type 400) spectroscopy as well as from the NH<sub>4</sub> exchange capacity measured by temperature-programmed ammonia evolution in the interval 453–923 K (Table 1).

The Gas Chromatographic Pulse Injection (GCPI) technique for *m*-xylene adsorption consisted of introduction of *m*-xylene vapor (0.16 kPa) in N<sub>2</sub> (60 ml/min) passing through a saturator equilibrated at 8 °C and introduced in a micro-flow adsorption bed loaded with 90 mg catalyst [31]. The breakthrough time and the relative *m*-xylene uptake at 40 °C are determined by continuously monitoring the exit *m*-xylene stream by means of FID detector of the GC unit.

Solid-state <sup>27</sup>Al MAS NMR experiments were carried out on Varian NMR System spectrometers at Larmor frequency of 104.4 MHz (B<sub>0</sub> = 9.4 T) and 156.4 MHz (B<sub>0</sub> = 14.1 T). Samples were packed into either 4.0 mm or 3.2 mm zirconia rotors, respectively. The magic angle spinning frequency (ν<sub>MAS</sub>: 13 kHz or 16 kHz) was set to avoid the spectral overlap of spinning sidebands. <sup>27</sup>Al chemical shifts are referred to Al(NO<sub>3</sub>)<sub>3</sub>(aq) using NaAlO<sub>2</sub> (δ<sub>27Al</sub> = 79.3 ppm) as secondary reference [32]. Fine calibration of the single pulse excitation experiment was carried out in case of the sample MCM-22 (optimal parameters: 2.5 μs excitation pulse and 5 s relaxation delay). The total experimental time was approximately 16 h for each sample. The spectral width was set to 625 kHz and 81920 complex points were acquired. The spectra were zero filled to 256,000 points and multiplied by an exponentially decaying function (lb = 20 Hz). The backward linear prediction processing method [33] was used to get rid of the baseline distortions. Quantitative analysis of the aluminum species was carried out by using the relative integrals of the relevant spectral regions. The precision of the method was increased by averaging the data determined from three spectra for each sample (number of scans: 5120, 10,240 and 15,360, respectively).

Quantitative analysis of the <sup>27</sup>Al MAS NMR spectra of the parent and steam-acid dealuminated materials were significantly

**Table 1**  
Aluminum content, ion-exchange capacity and textural properties of the samples.

Sample	Dealumination method		Aluminum content		IEC <sup>b,d</sup> (mmol/g)	Surface area <sup>b,e</sup> (m <sup>2</sup> /g)	Micropore volume <sup>b,f</sup> (cm <sup>3</sup> /g)
	Steaming	Acid reflux <sup>a</sup>	ΣAl <sup>b</sup> (mmol/g)	Proportion of the Al species <sup>c</sup> (%)			
MCM-22	–	–	1.08	95/–/5	0.96	578	0.18
D500	500 °C, 3 h	–	1.09	45/14/41	0.43	534	0.15
D500/Ox	500 °C, 3 h	Oxalic, 24 h	0.69	51/8/41	0.36	538	0.15
D500/Ox NH <sub>4</sub> <sup>+</sup> -form	–	–	0.66	74/4/22	–	–	–
D500/Ox H-form	–	–	–	53/7/40	–	–	–
D700	700 °C, 3 h	–	1.13	38/21/41	0.26	515	0.15
D700/Ox	700 °C, 3 h	Oxalic, 24 h	0.63	48/14/38	0.19	–	–
D700/HCl	700 °C, 3 h	HCl, 3 h	0.66	59/8/33	0.23	521	0.15
D800	800 °C, 3 h	–	1.14	35/21/44	0.19	–	–
D800/HCl	800 °C, 3 h	HCl, 3h-	0.65	47/12/41	0.19	481	0.14

<sup>a</sup> The acid reflux was carried out 373 K using either 0.5 M H<sub>2</sub>C<sub>2</sub>O<sub>4</sub> or 2 M HCl.

<sup>b</sup> All data were related to 1 g of sample, calcined at 973 K.

<sup>c</sup> The proportion of the different aluminum species were determined by integrating the <sup>27</sup>Al MAS NMR spectra (see Fig. 2). The sequence is: tetrahedral/5-coordinated or distorted tetrahedral/octahedral environments, respectively.

<sup>d</sup> The ion-exchange capacity (IEC) of the samples, obtained as the amount of ammonia, evolved from the NH<sub>4</sub><sup>+</sup> form sample in the 453–923 K temperature range during the TPAE run.

<sup>e</sup> Calculated by the multiple BET method from the N<sub>2</sub> adsorption isotherms.

<sup>f</sup> Estimated from the alpha-s plots.

influenced by the relaxation delay, if shorter than 5 s. The relative intensities of the resonances corresponding to the different coordination environments (Al species) were determined at 14 T in order to minimize the major source of inaccuracy because of the inability to detect all the aluminum species at low magnetic field [34].

### 2.3. Catalytic studies

The test reaction has been carried out in a fixed-bed flow reactor at atmospheric pressure, reaction temperatures of 523 K and 623 K and various contact times. N<sub>2</sub> carrier gas was passed through a saturator filled with *m*-xylene and equilibrated at 293.2 K so that partial pressure of 0.9 kPa to be attained. On-line analysis of the reaction products has been performed using HP–GC with 25 m FFAP capillary column.

### 2.4. Coke determination

Thermogravimetric microbalance (Setaram TG 92) experiments described in Ref. [35] were used for determination of the adsorbed carbonaceous species on the spent catalysts. The preparation procedure of the used catalysts included the following. The catalytic experiments were aborted after chosen time period (usually 120 min), the volatiles were eliminated by heating in N<sub>2</sub> for 30 min at the reaction temperature. Then the samples were cooled down still in N<sub>2</sub>, taken out from the reactor, placed in the microbalance and heated first in Ar by raising the temperature (10 K/min) up to 823 K. Then the flow of Ar was exchanged to air flow and the aged catalyst was left for another 1 h at 823 K. The registered weight loss corresponds to the amount of the intermediates and products desorbed up to 823 K in Ar, the so called “light coke”, and to that of the strongly held “hard coke” removed in air at 823 K.

## 3. Results and discussion

### 3.1. Physicochemical characteristics of the samples

The X-ray diffraction patterns (Fig. 1) show that between 5 and 15 2θ the intensity of the reflections for the samples steamed at 500 °C and 700 °C (D500 and D700) and their acid-treated varieties (D500/Ox, D700/Ox and D700/HCl) is higher than that of the parent MCM-22 material. The enhanced intensity of these reflections, according to Cambor et al. [36], can be due to the removal of Al

from lattice positions. The authors found out that the XRD pattern of ITQ-1, the pure silica analog of MCM-22, was better resolved than those of Al-MCM-22 and indicated an improved crystallinity. We suggest the same effect for our dealuminated materials with the exception of the most severely heated D800 and D800/HCl samples (Fig. 1). Some amorphization may have occurred as a result of the higher steaming temperature in this case. No diffraction peaks due to another crystalline phase were observed for our steamed and steamed/acid-leached materials.

Wu et al. [29] also reported comparable or even higher intensity of the XRD reflections of their steam-acid dealuminated materials compared to the corresponding parents.

The chemical composition, ion-exchange capacity and the textural properties of the parent and dealuminated samples are presented in Table 1. The difference between the total aluminum content (1.08 mmol/g) and the IEC (0.96 mmol/g) of the initial material indicates that about 11% of Al is in extra-framework positions. The amount of aluminum in the steamed samples D500, D700 and D800 remains similar to that of the parent material but their ion-exchange capacity decreases significantly by 60%, 77% and 83%, respectively. The results indicate that substantial portion of the Al

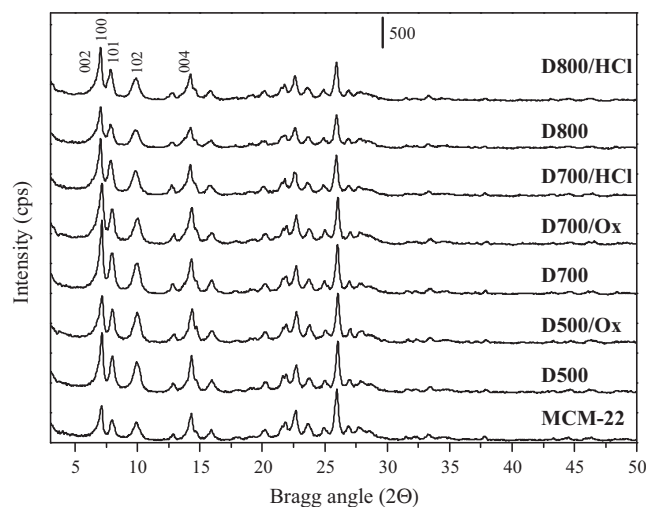


**Fig. 1.** XRD patterns of the parent, steamed and steamed/acid-leached MCM-22 samples.

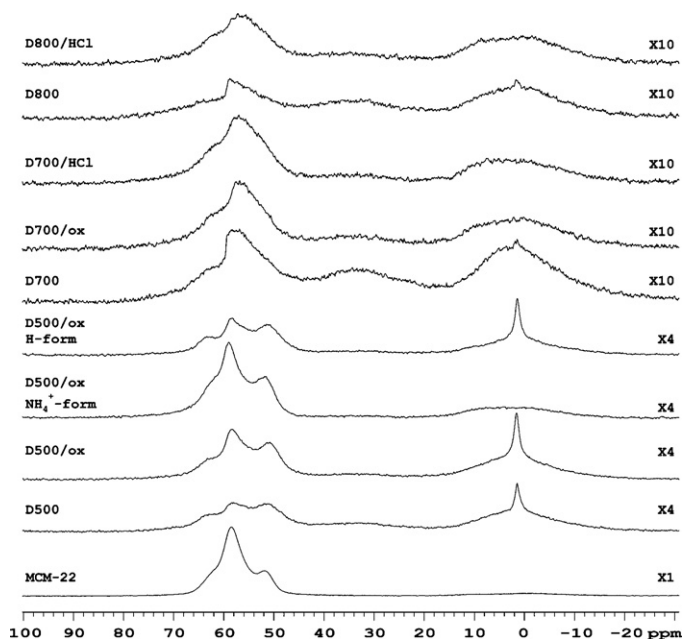


**Fig. 2.** Central region of the  $^{27}\text{Al}$  MAS NMR spectra of the parent, steamed and acid-treated MCM-22 samples. The value of magnification is indicated at the right side of each spectrum. The relative intensities of the resonances are given in Table 1.

atoms has been removed from tetrahedral positions, the higher the more rigorous the hydrothermal treatment has been.

The subsequent acid leaching results in a similar decrease, by about 40%, of the total Al content for all acid-treated materials. The results suggest that both extra-lattice and tetrahedrally coordinated aluminum atoms have been expelled from the zeolite structure upon the acid reflux (Table 1) and the total dealumination degree does not depend so much on the acid used.

### 3.1.1. $^{27}\text{Al}$ MAS NMR

Solid state  $^{27}\text{Al}$  MAS NMR spectroscopy has become an efficient method to determine the coordination state of the aluminum species in zeolites. The non-equivalent positions of identical aluminum coordination states may strongly overlap, but the resonances of tetrahedral and octahedral environments are sufficiently resolved to determine the Al(IV)/Al(VI) ratio, respectively [36]. The  $^{27}\text{Al}$  MAS NMR spectra of the parent and the steamed and steamed/acid-leached materials are shown in Fig. 2. Intense resonances at the high frequency region (ca. 70–50 ppm) were observed in case of all samples. These overlapping resonances are assigned to charge-balanced, tetrahedrally coordinated framework aluminum atoms. The gradual decrease and broadening of these signals is also accompanied by the appearance of another slight resonance at ca. 30 ppm (in particular for D700 and D800) attributed to either pentahedral or tetrahedrally-distorted Al species (framework Al interacting with  $\text{Al}^{n+}$ ) [38–40], all they generated as a result of steaming and slightly reduced after the acid reflux. A very weak resonance at ca. 0 ppm can be detected for the calcined parent zeolite (Fig. 2, MCM-22). Upon steaming at 500 °C a broad and a sharp resonance appear in the spectrum (Fig. 2, D500). The broad resonance is assigned to polymeric aluminum species [21,23], which cannot be removed by the following acid treatment (Fig. 2, D500/ox).

The sharp line at 0 ppm disappeared completely upon liquid phase ammonium ion exchange, whereas the resonances due to tetrahedral Al increased (Fig. 2, D500/ox  $\text{NH}_4^+$ -form). Transformation of this  $\text{NH}_4^+$ -form to H-form by thermal deammoniation results in the restoration of the sharp line at 0 ppm and the

intensity decrease of the resonances at the 70–50 ppm region. The above reversible change of octahedrally coordinated aluminum to tetrahedral species suggest that three-fold coordinated framework Al atoms with  $\text{SiO}^-$  defect sites could be formed upon hydrothermal treatment at 500 °C (see below in Scheme 1, route II).

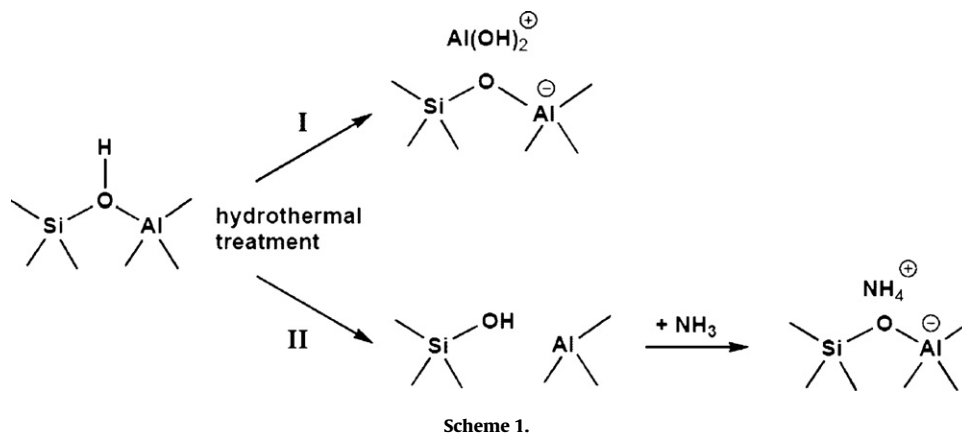
Calculations on the relative intensity of the signal of the peaks corresponding to the different Al species present in the steamed only and in the acid-refluxed materials were made. The results reveal (Table 1) that the various types of EFAl species formed during steaming and present in differing proportions of both essential kinds (in accordance to Fig. 2 and Ref. [40]) are only partially removed by acid treatment. From all dealuminated materials, the sample steamed at the lowest temperature and then refluxed with oxalic acid (D500/Ox) possesses the highest portion of tetrahedrally coordinated Al and the lowest percentage of extra-lattice aluminum. The most severe steaming generates the highest amount of EFAl on the expense of lattice aluminum which cannot be removed out of the zeolite structure by the subsequent acid leaching (D800/HCl). As a whole, about 10–20% of the aluminum atoms in the steamed materials that have been in tetrahedral positions restore their tetrahedral coordination after the acid reflux. This occurs on the expense of the 5-coordinated or distorted tetrahedral Al atoms, since the portion of the octahedrally coordinated Al remains practically unchanged (Table 1). The nonframework species, not able to be extracted by the acid (whatever they are), may: (i) compensate the framework charge of the zeolite resulting in a decrease in Brønsted acid site concentration [41], (ii) interact with part of the structural Al and consequently reduce their acid strength [42] or, finally, (iii) hinder the access to the effective acid sites by blocking the pores, as Xia et al. [23] have proposed. Each one of these possibilities seems probable as well for our steam-acid dealuminated materials, considering the consensus of all investigators on the presence of extractable EFAl in the lattice of the dealuminated MCM-22 zeolites, regardless of the applied procedure for their preparation.

### 3.1.2. FT-IR studies

In order to obtain information about the type of the acid sites in the parent, the steamed and the subsequently acid-treated materials, FT-IR spectra before and after Py adsorption were made (Fig. 3). The spectra in the hydroxyl stretching region show (Fig. 3A), that steaming results in a strong reduction (D500) or even in the disappearance (D700 and D800) of the band attributed to bridging OH groups ( $3620\text{ cm}^{-1}$ ). Simultaneously, an increase in the intensity of the external Si–OH groups ( $3745\text{ cm}^{-1}$ ) is observed. The following acid treatment step leads to an increased concentration of the internal silanols ( $3727\text{ cm}^{-1}$ ) on the expense of the external Si–OH ( $3745\text{ cm}^{-1}$ ) and to the appearance of new bands at  $3700\text{ cm}^{-1}$  and at  $3527\text{ cm}^{-1}$  in case of the acid-leached samples (Fig. 3A).

The band at  $3727\text{ cm}^{-1}$  is also registered by Meloni et al. [43] in MCM-22 materials with higher Si/Al ratio and corresponds to the “hydroxyl nests” detected on steamed [21], acid-leached [13] or steam and acid-treated [29] zeolites of the MCM-22 type. In our case the intensity of the band at  $3727\text{ cm}^{-1}$  is the highest for the most severely steam-treated D800/HCl.

The new bands appeared at  $3700\text{ cm}^{-1}$  and  $3527\text{ cm}^{-1}$  after acid reflux of the steamed samples are ascribed by Corma et al. [15] and Meloni et al. [43], to the particular, also internal silanols (defect sites), located preferentially in the supercages and 10 MR sinusoidal channels, respectively. Their concentration is again the highest for D800/HCl. The broad band around  $3500\text{ cm}^{-1}$  detectable in the FT-IR spectra of D700/Ox, D700/HCl and D800/HCl (Fig. 3A) is also observed in ZSM-5 zeolite and is ascribed to silanols interacting through hydrogen bonding [44,45]. The strong intensity reduction of the  $3620\text{ cm}^{-1}$  band attributed to the bridging OH groups or its complete disappearance for the more severe steam-treated



materials could be ascribed to the removal of practically all tetrahedral Al atoms. This observation is in contrast to our  $^{27}\text{Al}$  MAS NMR results (Fig. 2) that proved the presence of tetrahedral Al in all dealuminated materials. Our explanations for this contradiction are that, as a result of the dealumination, (i) part of the bridging OH groups was neutralized by cationic extra-lattice Al species (route I in Scheme 1) and (ii) the remained tetrahedral framework Al was transformed to tri-coordinated lattice aluminum (route II in Scheme 1), in accordance to the mechanism suggested by Altwasser et al. [46].

The authors also assume that  $\text{NH}_3$  can coordinate to these threefold-coordinated Al atoms and heals the framework Si–O–Al $^{(-)}$  bridges (Scheme 1). The latter suggestion explains why our steamed as well as acid-treated materials still possess some ion-exchange capacity (Table 1), but in the same time the bridging hydroxyls are practically missing in their FT-IR spectra.

In case of the initial sample pyridine adsorption causes the disappearance of the band at  $3620\text{ cm}^{-1}$  (not shown) and the appearance of the characteristic pyridinium band at  $1543\text{ cm}^{-1}$  (Fig. 3B). For the steamed materials the intensity of the pyridinium band is significantly lower than that of the initial MCM-22 samples, and further reduces for the samples undergone acid leaching. Py adsorption also leads to a small intensity decrease of the bands at  $3700\text{ cm}^{-1}$  and at  $3727\text{ cm}^{-1}$ .

Strong bands attributed to Py coordinated to Lewis acid sites also appear at  $1453\text{ cm}^{-1}$  and  $1446\text{ cm}^{-1}$  in case of the parent

zeolite. The intensity of these Lewis-connected Py bands is a bit higher for D500 and decreases with the steaming temperature. Acid treatment leads to partial extraction of this type of adsorption sites (D500/Ox) or to a change in their distribution (D700/HCl/Ox and D800/HCl) (Fig. 3B).

FT-IR spectra of Py adsorbed on only acid-leached MCM-22 zeolites [13] and on steamed mordenites [12] reveal much lower density of acid sites than the concentration of lattice Al atoms in their structure. The authors ascribe this phenomenon to a confinement effect within the micropores caused by the EFAl entities deposited during the dealumination procedure which restrict the access of the Py molecules to the zeolite acid sites. The same effect cannot be ruled out in our case, too.

The difficulty in removing these EFAl species out of the zeolite pores can be explained by the  $^{27}\text{Al}$  MAS NMR results of Meriaudeau et al. [21] and Ma et al. [22] on hydrothermally treated MCM-22 materials. These authors claim that deeper steam dealumination occurs at higher temperatures and the aggregation and condensation of the expelled octahedral extra-framework aluminum atoms into polymeric aluminum species takes place at vigorous steaming. If such species have been formed at  $700^\circ\text{C}$  and  $800^\circ\text{C}$  compared to  $500^\circ\text{C}$  in our case, then they are supposed to be eliminated with more difficulty by the next acid reflux, as our experiments indeed have shown. Milder steaming generates not aggregated [21] and monomeric Al species [22] that should be more easily extractable by the subsequent acid treatment.

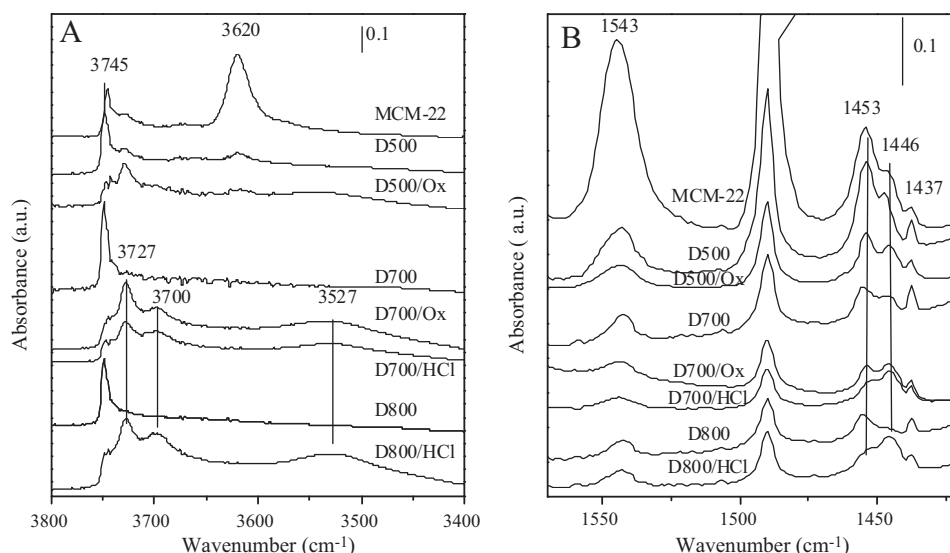


Fig. 3. FT-IR spectra of the parent and dealuminated samples (A) after evacuation at 673 K for 1 h and (B) after Py adsorption at 473 K and evacuation at 473 K for 0.5 h.

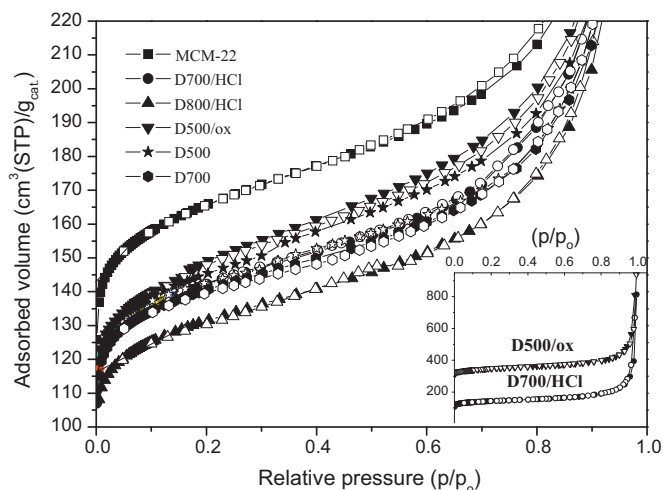


Fig. 4.  $N_2$  adsorption and desorption isotherms of the parent MCM-22 zeolite, the steamed and the consecutively steam-acid dealuminated zeolites.

Results suggest that steam treatment of MCM-22 leads to reduction of the framework Al atoms and formation of octahedrally and pentahedrally coordinated EFAl species. The successive acid treatment results in additional but only partial (40%) extraction of both framework and extra-framework aluminum.

### 3.1.3. Adsorption studies

The proposal about pore blockage by EFAl species in zeolite MCM-22 treated by nitric acid only have been presumed before by Matias et al. [13] but declined back by the authors themselves with the argument that "...such proposal could seem surprising when the nitrogen adsorption data are considered". This conclusion is based on the absence of change in the micropore volume after the acid treatment of the parent zeolite. The same argument against the possibility of micropore blocking by EFAl species is given by Wu et al. [29] considering the slight changes in the micropore volume of the steam-acid dealuminated materials compared to the parent one. In both contributions, however, the micropore volume is measured not with an adsorbate with a similar size of the reactant molecule but with small  $N_2$  molecule [13]. Not to neglect this very important consideration, adsorption experiments not only with  $N_2$  but also with the *m*-xylene reactant have been performed in the present investigation.

**3.1.3.1.  $N_2$  adsorption.** In Fig. 4 the  $N_2$  adsorption and desorption isotherms of the parent, steamed and steamed/acid-leached samples are presented. As the data show, the decrease in the micropore volume for the mildly steam-acid treated samples (D500, D500/Ox) determined by  $N_2$  adsorption is about 17% (Table 1). The micropore volume of the sample hydrothermally treated at 800 °C is the lowest (Fig. 4). Comparing the isotherm of the steamed (D500, D700, D800) and subsequently acid-treated samples, it can be concluded that upon acid reflux the micropore volume of the samples practically does not change. Results suggested that the lower  $N_2$  adsorption capacity of the dealuminated zeolites is not due to the loss of crystallinity considering the even higher intensity of the XRD reflections of the dealuminated samples (with the exception of D800/HCl, Fig. 1), but rather to the presence of EFAl entities inside the pores, causing some adsorption limitations even for the small  $N_2$  molecule. BET surface area decreases also, not substantially, as a result of dealumination (Table 1). The absence of hysteresis of the isotherms (inset in Fig. 4) proved that mesopores were not formed even after acid leaching.

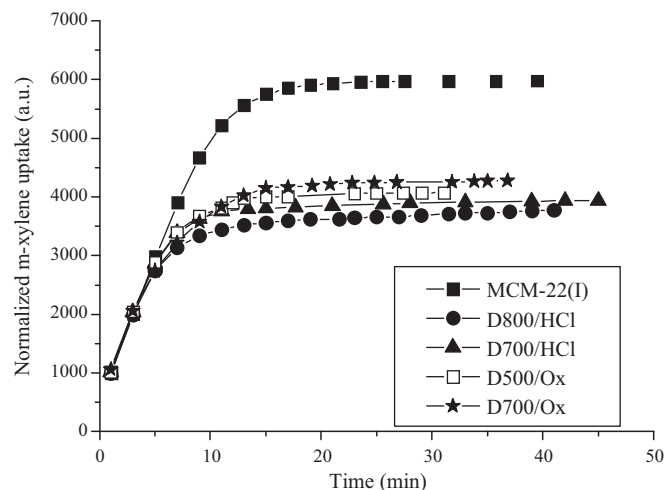


Fig. 5. Uptake curves of *m*-xylene adsorption at 313 K over the parent MCM-22 and the steam-acid dealuminated materials.

**3.1.3.2. *m*-Xylene uptake.** On Fig. 5 the *m*-xylene uptake over the initial and the steam-acid dealuminated materials in dependence on the adsorption time measured by GCPI technique was presented. As the figure reveals, the adsorption capacity of the dealuminated samples amounts to about 62–70% of that of the parent MCM-22 depending on the severity of the dealumination procedure. Same sequence in the capacity decrease for  $N_2$  and *m*-xylene adsorption is found on the steamed and acid treated samples but the uptake decrease for the bigger *m*-xylene molecule is larger than that of nitrogen. The most rigorously steam-acid dealuminated D800/HCl displays the lowest adsorption capacity for both  $N_2$  and *m*-xylene. Diffusional barriers caused by the EFAl species remained deposited after both stages of dealumination should be responsible for the observed reduction in the adsorption capacity.

Analogously, reduced capacity towards *n*-hexane and more markedly for the bigger cyclohexane molecule has been observed by Ding et al. [47] on only steamed ZSM-5 compared to the starting material. The authors also found lower total pore volume as well as lower micropore area and volume for the hydrothermally treated samples but they attribute this effect to the narrowing of the zeolite channels as a result of the replacement of the longer Al–O bonds by the shorter Si–O bonds.

### 3.2. *m*-Xylene transformation

The catalytic properties of the parent material were compared to that of its dealuminated modifications obtained at each dealumination steps, steaming and subsequent acid reflux, respectively. Whatever the reaction temperature and the contact time applied, the products expected from *m*-xylene isomerization (*p*- and *o*-isomer) and disproportionation (toluene and trimethylbenzenes) are observed. The conversion on the steamed at 773 K and 973 K and their acid-treated modifications (Fig. 6A and B, respectively) together with the parent, are presented as a function of the time on stream (TOS). In accordance with the loss of framework Al atoms and respectively of Brønsted acid sites (IEC, FT-IR and  $^{27}\text{Al}$  MAS NMR data) the samples reveal decreasing catalytic activity after the consecutive steps of steaming and acid leaching, compared to the parent material. The activity of the more severely steamed catalysts as well as those of their acid-leached modifications is much lower.

The vastly reduced catalytic activity of the dealuminated materials compared to their parent corresponds to the loss of accessible acid sites detected by the FT-IR measurements of adsorbed Py

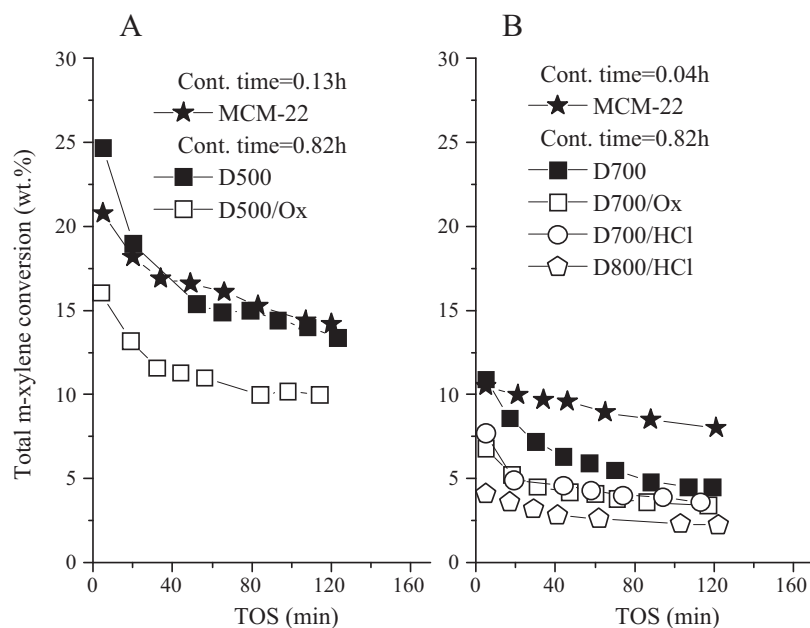


**Fig. 6.** Total *m*-xylene conversion as a function of the TOS for the dealuminated catalysts steamed at 773 K (A), and at 973 K (B), and subsequently acid refluxed. Reaction temperature 623 K.

(Fig. 3B) and is in accordance with the reduction in their *m*-xylene adsorption capacity (Fig. 5). The sequence in the diminish of the activity follows the severity of steaming both for the steamed and acid leached catalysts (Fig. 6) and corresponds to the one ascertained by the Py and *m*-xylene adsorption measurements. These observations indicate that part of the EFAl species generated upon steaming and remained not extracted by the subsequent acid treatment are most probably responsible for the substantial loss of acid sites by both neutralizing part of them and giving rise to limitations in the access of the reactant molecule to the rest.  $^{29}\text{Si}$  MAS NMR studies of highly siliceous MCM-22 prepared by hydrothermal dealumination confirm the presence of at least one buried T-site per unit cell that is not accessible to a channel wall [37].

It turns out that the second stage of dealumination, the acid reflux, instead of increasing the Brønsted acidity as it happens with the steam-acid dealuminated mordenites, provokes like in beta zeolite (Ref. [12]), only partial removal of the EFAl species generated upon the previous steaming. The remaining, not effectively dislodged and most probably polymerized EFAl species may block the acid sites, whereas the cationic-type aluminum may endure re-dispersion and may neutralize part of these sites in accordance to Fernandes et al. [12]. If such process of aluminum redistribution occurs in the large pore zeolites, it should be more reinforced by the acid attack in the narrow 10 MR sinusoidal channels and the 10 MR openings of the supercages of zeolite MCM-22. Thus, it should result in additional reduction of the concentration and accessibility of the remaining Brønsted acid sites.

It is worth mentioning here, that the type of the acid used for reflux does not affect the catalytic action considering the behavior of both materials steamed at 973 K and subsequently treated with HCl or oxalic acid (Fig. 6B). Contrary to this, substantial difference is observed by Xia et al. [23] in the acidity as well as in the selectivity to dimethyl ether produced from syngas when direct treatment by individual acids (oxalic or citric) is applied on MCM-22. Our characterization results above indicate however, that when preliminary steaming step is applied, the type of the acid used upon the next reflux procedure appears to be insignificant. The severity of steaming determines preferentially the content and likely the type

of both lattice and extra-lattice Al present in the steamed samples. The proportion between the rest of them, left after the acid reflux, do not change significantly and does not depend on the type of the acid used. This result points to the contribution of each individual dealumination step, the steaming one being more essential.

In order to assess the selectivity of the catalysts, it was indispensable to apply quite differing reaction conditions for to attain close degree of *m*-xylene conversion on the parent and the dealuminated materials. In Fig. 7 the conversion and the *p*- to *o*-xylene ratio in dependence on the TOS are presented for diverse contact times and reaction temperatures. As the data show, whatever the reaction conditions and the dealumination procedure applied, at the adjusted close or equal conversion, the selectivity towards the *p*-xylene isomer is higher in case of the dealuminated catalysts and increases in the course of the reaction compared to that of the parent material. It is obvious that the observed effect is not a consequence neither from the difference in the reaction temperatures nor from the prolonged contact times, since longer contact times (used for the dealuminated catalysts) must facilitate the equilibration between the three isomer products which was not the case in our experiments.

Wu et al. [29] and Park et al. [27,28] also observed enhanced *p*-isomer selectivity in the reactions of toluene and ethylbenzene transformations respectively, for consecutively steam-acid dealuminated MCM-22 zeolites. According to these authors, the selective replacement of framework Al from the sinusoidal channels and the surface cups [29] or their preferential removal only from the external surface [27,28] suppresses the secondary isomerization of the primarily formed *p*-methyl/ethyl substituted benzenes and this is the reason for their enhanced fraction in the final product. The suggestion of Wu et al. [29] about the capability for a specific and more intense replacement of aluminum atoms from the sinusoidal channels of MCM-22 upon steam-acid dealumination appears somewhat doubtful, however, considering the last results of Matias et al. [13]. Following the change in the activity of the dealuminated by  $\text{HNO}_3$  zeolite MCM-22 in the test reaction of methylcyclohexane transformation these authors found out that the Al atoms are extracted first from the outer cups, and then

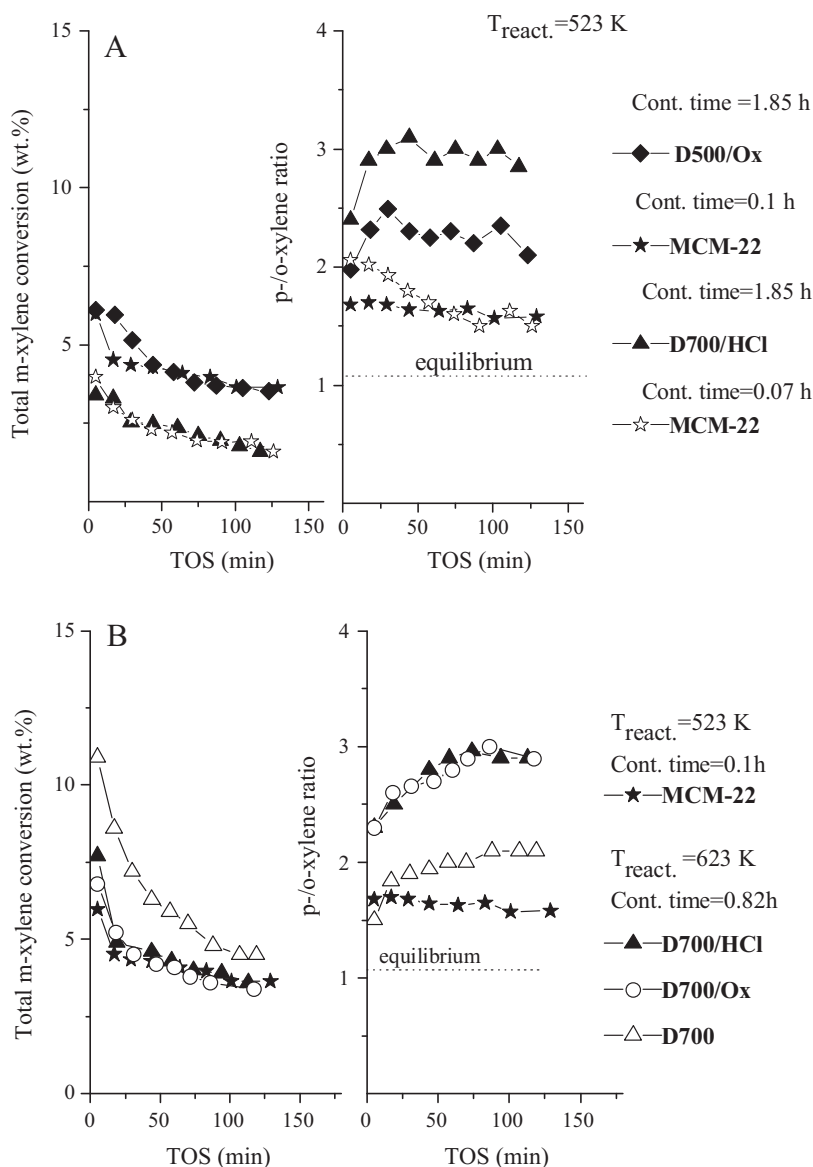


**Fig. 7.** *m*-Xylene conversion and *p*- to *o*-xylene ratio in dependence on the TOS at different contact times and reaction temperature of 523 K (A), 523 K and 623 K (B) for the parent and dealuminated catalysts.

preferentially from the larger supercages. The narrow sinusoidal channels are hardly affected by the acid because of diffusion limitations for the transport of the  $\text{HNO}_3$  molecules alone. Considering the succession of the steam-acid treatment in our case, even more embarrassed transport of the acid molecules together with the dissolved aluminum species, generated during the preceding hydrothermal treatment, might be expected, compared to the solely acid leaching. The acid molecules will suffer in our case of even more impeded diffusion through the micropores obstructed by the EFAl debris, especially when the most confined sinusoidal channels are considered. The lattice Al atoms located there should be the most unlikely to be extracted upon the next acid reflux.

Considering the significant decrease in the catalytic activity of our dealuminated catalysts presented above and their lower *m*-xylene adsorption capacity (Fig. 5), we rather suggest inaccessibility but not a selective extraction of framework Al from the sinusoidal channels. Matias et al. [13] also ascribe the diminish in the activity in methylcyclohexane transformation not only to the proton concentration decrease by partial extraction of the framework aluminum (by acid only in their case) but also to the limitation in

the access of the reactant molecules to these acid sites caused by the presence of the EFAl barriers. Thus the Wu's suggestion about the increased *p*-xylene selectivity of the steam-acid dealuminated MCM-22 should be a little bit modified in accordance to our experimental results. The higher *p*-selectivity might be indeed determined by the reduced number of acid sites in the sinusoidal channels, which, however, are not extracted by the acid leaching but are inaccessible because of the pore/site blockage by EFAl generated upon steaming. Dilution of the surface acid sites should also have occurred since the most accessible centers must be the most affected by the acid attack [13].

Since the acid treatment is not able to withdraw out of the narrow MCM-22 channel system all the EFAl entities generated by steaming, then these entities would remain captured within the zeolite micropores. This may cause, as well, diffusional limitations for the bulkier *o*-isomer and will reinforce shape selectivity effect in *m*-xylene transformation. This assumption is supported by the reduced adsorption capacity towards *m*-xylene determined above (Fig. 5) which should be due to blocking of the sinusoidal channels and/or narrowing of the 10 MR openings of the supercages

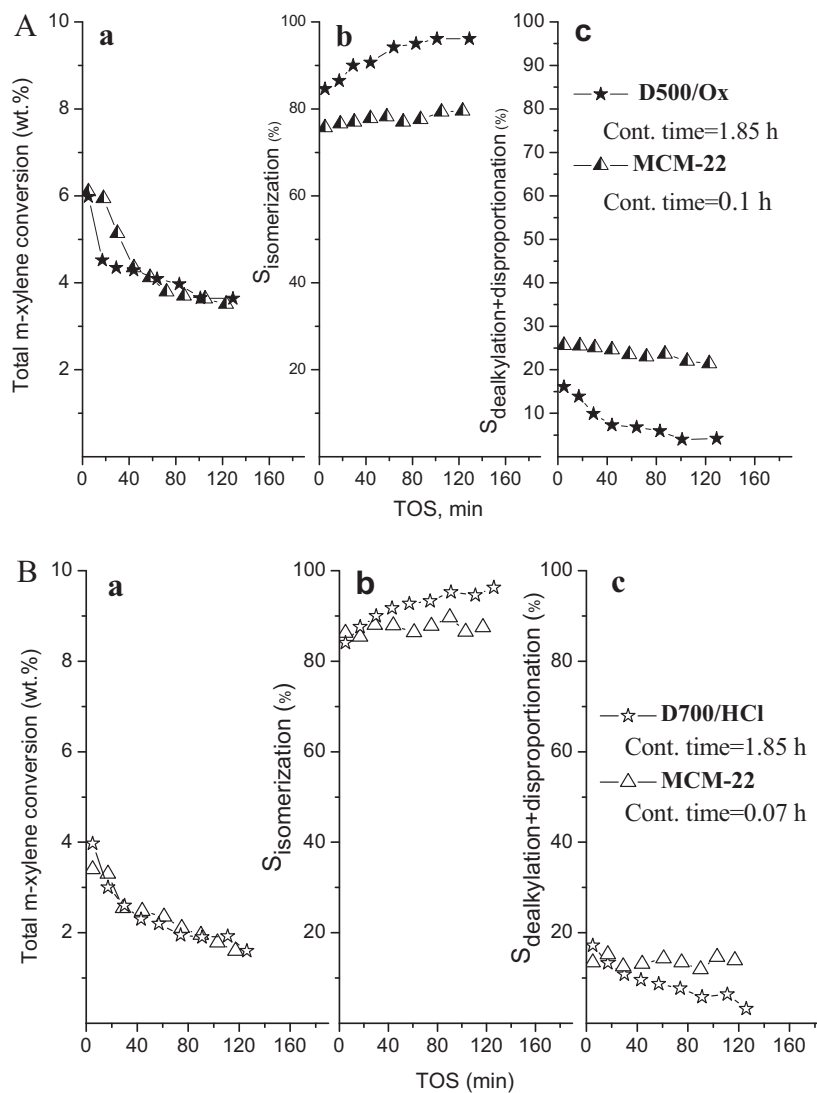


**Fig. 8.** Total *m*-xylene conversion (a), selectivity to isomerization (b), and to side reactions of *m*-xylene transformation (c), in dependence on the time on stream on D500/Ox (A) and D700/HCl (B) (contact time = 1.85 h) compared with MCM-22 (contact time = 0.1 and 0.07 h) at  $T_{\text{react}} = 523$  K.

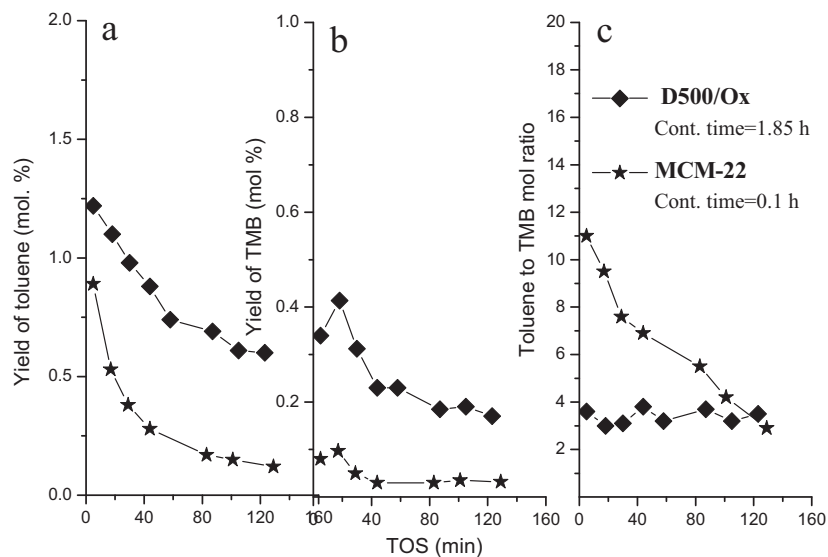


**Fig. 9.** Distribution of toluene and TMB reaction products over D500/Ox and MCM-22 at close total *m*-xylene conversion (depicted in Fig. 8) in dependence on the TOS. ( $T_{\text{react}} = 523$  K, cont. time = 1.85 h for D500/Ox and 0.1 h for MCM-22).

where *m*-xylene isomerization preferentially occurs [48]. It is in accordance, as well, to the selectivity effect revealed by hydrothermally dealuminated MCM-22 zeolites in the reaction of *n*-octane hydroconversion [21].

It should be noticed here that the *p*- to *o*-isomer ratio of the dealuminated catalysts increases with TOS (Fig. 7), an effect not mentioned and discussed by others studied the *p*-selectivity in the conversions of alkyl substituted aromatics [27–29]. This effect appears to be related to the deactivation of the dealuminated catalysts and may evolve from the gradual elimination of the remained acid sites by carbonaceous compounds. Coke precursors may also build up additional diffusion barriers, reduce the proton concentration and suppress the secondary isomerization of the primarily formed and most rapidly diffusing *p*-xylene isomer.

A different mode of deactivation of the parent material and its dealuminated modifications can be suggested in accordance to the observed reaction products distribution discussed below. In Fig. 8 the selectivity towards the isomerization ( $S_{\text{iso}}$ ) and the side reactions, i.e. dealkylation and disproportionation ( $S_{\text{dealk} + \text{dispr.}}$ ), at almost equal degree of *m*-xylene conversion for two steam-acid dealuminated catalysts is compared to their parent. Two main distinctions in the performance of both types of catalysts can be seen: (i) the selectivity towards the side reactions of *m*-xylene conversion of the parent material decreases with the TOS on the expense of its isomerization and that corresponds to the deactivation rate. In case of the dealuminated catalysts the values for  $S_{\text{iso}}$  and  $S_{\text{dispr.}}$  remain almost constant, and (ii) the dealuminated samples reveal lower selectivity towards isomerization and higher for disproportionation compared to their parent.

According to Laforge et al. [49], the deactivation of the catalysts of the MCM-22 type upon *m*-xylene conversion reflects the decrease in the intensity of disproportionation which occurs on the acid sites located in the supercages where coke preferentially accumulates. This process is associated with the pore blocking effect strongly pronounced for these so called “trap cages” (large cages with small apertures) of MCM-22 [50], according to the classification of Guisnet et al. [51]. Our parent material displays analogous performance (Fig. 8A and B). If one considers the confined space in the large supercages of our steam-acid dealuminated catalysts, however, then *m*-xylene disproportionation (which involves bulky bimolecular intermediates) should occur exceptionally at the acid sites remaining on the external hemicages. The deactivation of these surface sites should be due to “site poisoning” rather than to “pore blockage” (Ref. [51]) and should lead to a proportional and constant change in the selectivity of both isomerization and disproportionation as our results actually show. Desorption of the bulk disproportionation products (TMB isomers) from these large external cups with small depth would be easier and faster, and their retention time should be shorter enough to prevent substantial secondary transformations [52] as it is shown below.

Comparison of the side products distribution on both types of catalysts, parent and dealuminated, supports the suggestion made above. Larger yields of toluene and TMB are detected on D500/Ox (Fig. 9a and b) which indicates facilitated reaction of *m*-xylene disproportionation over the dealuminated catalyst. The Tol:TMB mole ratio is constant (Fig. 9c) however, and amounted to 3 indicating some permanent loss of TMB isomers, but much lower than that of the parent material (starting from 11 and decreasing along with the catalyst deactivation). This much higher selectivity in favor of toluene (Fig. 9c) is accompanied by formation of ethyltoluene and C<sub>2</sub>–C<sub>4</sub> hydrocarbons (not shown). This is an indication for more intense occurrence of secondary reactions of transformation of the TMB molecules remained trapped in the “empty” micropores of this catalyst. Such a process is strongly restricted by the presence of EFAL entities in the channel system of the dealuminated materials.

**Table 2**

Weight loss determined by TGA upon heating in Ar from room temperature to 873 K and kept in air for 1 h at 873 K.

Samples	Heating in Ar				Heating in air At 873 K	Total loss Over 498 K (Ar + air), %
	303–498 K		498–873 K			
	$T_{\text{max}}$	% Loss	$T_{\text{max}}$	% Loss	% Loss	
MCM-22	368 K	7.1	709 K	0.5	1.89	2.35
D500/Ox	363 K	3.7	831 K	1.31	0.11	1.42

The disproportionation reaction of *m*-xylene should occur not inside the narrowed pores but preferentially and more facilitated on the surface hemycages. Then gradual elimination by progressive coke formation on the remaining there acid surface sites starts, most probably by the site poisoning mechanism of deactivation proposed by Guisnet et al. [51]. In the same time, the deactivation rate of both catalysts is analogous (Fig. 8a).

The results from the coke determinations for the couple of spent catalysts MCM-22 and D500/Ox which reveal same degree of *m*-xylene conversion and deactivation rate (Fig. 8a) are presented in Table 2. In accordance with the interpretations of Bibby et al. [53] and Pradhan et al. [54], three well established peaks of water elimination (303 K–498 K, not shown), and replacement of the more mobile carbonaceous deposits—“soft” coke (498–873 K) are detected in argon flow. The strongly retained, more condensed compounds considered as “hard” coke are liberated upon air combustion at 873 K. According to the data, the dealuminated catalyst is able to adsorb twice lower amount of H<sub>2</sub>O, and its total weight loss is also about half of its parent, most probably because of the restricted void pore volume. The highly volatile coke precursors released from it in argon, at the high temperature interval (498–873 K), are about three times higher, than that of the parent. On the contrary, the parent material reveals preferential formation of much more condensed coke deposits eliminated in air. Obviously, the composition of the coke over the parent and the dealuminated catalysts differ in a great extent. The more condensed deposits on the former are probably accumulated into the supercages as was suggested above. These compounds are strongly embarrassed to leave the “trap cages” and endure intense condensation. Higher temperature and air flow are needed for their removal from the aged catalyst. In contrast, coke precursors on the dealuminated materials comprises of more volatile compounds, since they grow on the surface cups and can readily desorb from there, at lower temperature and still in Ar. The process of formation of these coke precursors is determined by the larger space available on the external surface of the dealuminated catalysts, independently from the much longer contact time applied for the catalytic experiments with them.

Thus, it can be suggested that the disposition of the residual EFAL in the three different pore systems of MCM-22 affects the reaction products distribution in both reactions of isomerization and disproportionation in *m*-xylene transformation, as well as it determines the mechanism of carbonaceous compounds formation. This observation is in accord to the conclusion of Guisnet et al. [51] that both coke formation and deactivation are shape-selective processes.

#### 4. Conclusion

The effect of the residual EFAL species can be generalized as follows:

1. The presence of EFAL entities causes blocking of the zeolite micropores and leads to significant reduction in their adsorption capacity and catalytic activity. This effect is assumed to be a particular feature of the steam-acid dealuminated MCM-22.

2. The proposed by other authors selective replacement of proton sites by such steam-acid dealumination of MCM-22 zeolite should be implied not only as definite extraction and elimination of the framework Al atoms connected to bridging protons but also as a process of “burying” of these acid sites under the EFAl species. This makes most of the proton sites inaccessible and inefficient and is the reason for the observed enhanced *p*-xylene selectivity.
3. The presence of residual EFAl species limits the access of the reactant molecules to the catalytically active sites, leads to reduced activity in *m*-xylene conversion, affects the products distribution in both reactions of *m*-xylene isomerization and disproportionation and determines the mode of coke formation.

## Acknowledgments

Support of this work in the framework of the Hungarian-Bulgarian Inter-Academic Exchange Agreement (project no. 17) is gratefully acknowledged. The support of the Hungarian GVOP-3.2.1.-2004-04-0210/3.0 grant is gratefully acknowledged.

## References

- [1] J. Cejka, A. Corma, S. Zones (Eds.), *Zeolites and Catalysis. Synthesis, Reactions and Applications*, Wiley-VCH Verlag GmbH&Co. KGaA, Weinheim, 2010.
- [2] (a) C. Choifeng, J.B. Hall, B.J. Huggins, R.A. Beyerlein, *J. Catal.* 140 (1993) 395–405;  
(b) R.A. Beyerlein, C. Choi Feng, J.B. Hall, B.J. Huggins, G.J. Ray, *Top. Catal.* 4 (1997) 27–42.
- [3] A. Corma, V. Fornes, F. Rey, *Appl. Catal.* 59 (1990) 267–274.
- [4] J. Scherzer, *ACS Symp. Ser.* 248 (1984) 157–200.
- [5] J. Linch, F. Raatz, P. Dufresne, *Zeolites* 7 (1987) 333–340.
- [6] J.L. Molz, H. Heinichen, W.F. Holderich, *J. Mol. Catal. A: Chem.* 136 (1998) 175–184.
- [7] C.S. Triantafillidis, A.G. Vlessidis, L. Nalbandian, N.P. Evmiridis, *Microporous Mesoporous Mater.* 47 (2001) 369–388.
- [8] G.C. Groen, J.A. Moulijn, J. Perez-Ramirez, *Microporous Mesoporous Mater.* 87 (2005) 153–161.
- [9] M.R. Minas, I. Rahmim, A.S. Fung, J.R.A. Huss, US Patent 5321194 (1994).
- [10] M.R. Apelian, A.S. Fung, J.K. Gordon, F. Thomas, *Prepr. 14th North American Meeting of the Catalysis Society, Snowbird, Utah, 1995*.
- [11] M. Muller, G. Harvey, R. Prince, *Microporous Mesoporous Mater.* 34 (2000) 135–147.
- [12] L.D. Fernandes, J.L.F. Monteiro, E.F. Sousa-Aguilar, A. Martines, A. Corma, *J. Catal.* 177 (1998) 363–377.
- [13] P. Matias, J.M. Lopes, P. Ayrault, S. Laforge, P. Magnus, M. Guisnet, F. Ramoa Ribeiro, *Appl. Catal. A: Gen.* 365 (2009) 207–213.
- [14] M.E. Leonowicz, J.A. Lawton, S.L. Lawton, M.K. Rubin, *Science* 264 (1994) 1910–1913.
- [15] A. Corma, C. Corell, J. Perez-Pariente, *Zeolites* 15 (1995) 2–8.
- [16] A. Corma, C. Corell, V. Fornes, W. Kolodziejewski, J. Perez-Pariente, *Zeolites* 15 (1995) 576–582.
- [17] S.M. Campbell, D.M. Bibby, J.M. Coddington, R.F. Howe, R.H. Meinhold, *J. Catal.* 161 (1996) 338–349.
- [18] T. Masuda, Y. Fujikata, S.R. Mukai, K. Hashimoto, *Appl. Catal. A: Gen.* 172 (1998) 73–83.
- [19] P. Canizares, A. Carrero, *Appl. Catal. A: Gen.* 248 (2003) 227–237.
- [20] L. Teyssier, M. Thomas, C. Bouchy, J. Martens, E. Guillon, in: A. Gedeon, P. Masiani, F. Baboneau (Eds.), *Zeolites and related materials: Trends, Targets and Challenges*, *Stud. Surf. Sci. Catal.*, vol. 174, Elsevier, Amsterdam, 2008, p. 969.
- [21] P. Meriaudeau, Vu A. Tuan, Vu T. Nghiem, F. Lefevre, Vu T. Ha, *J. Catal.* 185 (1999) 378–385.
- [22] D. Ma, F. Deng, R. Fu, X. Han, X. Bao, *J. Phys. Chem. B* 105 (9) (2001) 1770–1779.
- [23] J. Xia, D. Mao, W. Tao, Q. Chen, Y. Zhang, Y. Tang, *Microporous Mesoporous Mater.* 91 (2006) 33–39.
- [24] S. Unverricht, M. Hunger, S. Ernst, H.G. Karge, J. Weitkamp, in: J. Weitkamp, H.G. Karge, H. Pfeifer, W. Holderich (Eds.), *Zeolites and Related Microporous Materials, State of the Art 1994*, *Stud. Surf. Sci. Catal.*, vol. 84, Elsevier, Amsterdam, 1994, p. 37.
- [25] X. Ren, J. Liang, J. Wang, *J. Porous Mater.* 13 (2006) 353–357.
- [26] J.-N. Park, J. Wang, S.-I. Hong, C.W. Lee, *Appl. Catal. A: Gen.* 292 (2005) 68–75.
- [27] S.-H. Park, H.-K. Rhee, *React. Kinet. Catal. Lett.* 78 (2003) 73–80.
- [28] S.-H. Park, H.-K. Rhee, *Appl. Catal. A: Gen.* 219 (2001) 99–105.
- [29] P. Wu, T. Komatsu, T. Yashima, *Microporous Mesoporous Mater.* 22 (1998) 343–356.
- [30] R. Ravishankar, D. Bhattacharya, N. Jacob, S. Sivasankar, *Microporous Mesoporous Mater.* 4 (1995) 83–93.
- [31] R.M. Mihályi, I. Kolev, V. Mavrodinova, M. Kollár, T. Korányi, Ch. Minchev, in: K. Hadjiivanov, V. Valtchev, S. Mintova, G. Vayssilov (Eds.), *Advanced Micro- and Mesoporous Materials*, Heron Press, 2008, pp. 363–371.
- [32] D.L. Bryce, G.M. Bernard, M. Gee, M.D. Lumsden, K. Eichele, R.E. Wasylshen, *Can. J. Anal. Sci. Spectrosc.* 46 (2001) 46–82.
- [33] P. Koehl, *Progress NMR Spectrosc.* 34 (1999) 257.
- [34] T.H. Chen, B.H. Wouters, P.J. Grobet, *Eur. J. Inorg. Chem.* (2000) 281–285.
- [35] V. Mavrodinova, M. Popova, Y. Neinska, Ch. Minchev, *Appl. Catal. A: Gen.* 210 (2001) 397–408.
- [36] M.A. Cambor, A. Corma, M.J. Dias-Cabanas, *J. Phys. Chem. B* 102 (1998) 44–51.
- [37] G.J. Kennedy, S.L. Lawton, A.S. Fung, M.K. Rubin, S. Steuernagel, *Catal. Today* 49 (1999) 385–399.
- [38] A. Corma, V. Fornes, A. Martinez, J. Sanz, *ACS Symp. Ser.* 375 (1988) 17–33.
- [39] J.P. Gilson, G.C. Edwards, A. Petes, K. Rajagopalan, R.F. Wormsbecher, T.G. Roberie, M.P. Shatlock, *J. Chem. Soc. Chem. Commun.* (1987) 91–92.
- [40] N. Malicki, G. Mali, A.-A. Quoineaud, P. Bourges, L. Simon, F. Thibault-Starzyk, C. Fernandez, *Microporous Mesoporous Mater.* 129 (2010) 100–105.
- [41] A. Corma, A. Martinez, C. Martinez, *Appl. Catal. A: Gen.* 134 (1996) 169–182.
- [42] J. Miller, P. Hopkins, B. Meyers, G. Ray, R. Roginski, G. Zajac, N. Rosenbourn, *J. Catal.* 138 (1992) 115–128.
- [43] D. Meloni, S. Laforge, D. Martin, M. Guisnet, E. Rombi, V. Solinas, *Appl. Catal. A: Gen.* 215 (2001) 55–66.
- [44] M.S. Holm, S. Svelle, F. Joensen, P. Beato, C.H. Cristensen, S. Bordiga, M. Bjorgen, *Appl. Catal. A: Gen.* 356 (2009) 23–30.
- [45] C. Fernandez, I. Stan, J.-P. Gilson, K. Thomas, A. Vicente, A. Bonilla, J. Perez-Ramirez, *Chem. Eur. J.* 16 (2010) 6224–6233.
- [46] S. Altwasser, J. Jiao, S. Steuernagel, J. Weitkamp, M. Hunger, in: E. van Santen, L. Callanan, M. Claeys (Eds.), *Proc. 14th Int. Zeol. Conf.*, Cape Town, 2004, pp. 1212–1213.
- [47] C. Ding, X. Wang, X. Guo, S. Zhang, *Catal. Commun.* 9 (2007) 487–493.
- [48] S. Laforge, D. Martin, M. Guisnet, *Microporous Mesoporous Mater.* 67 (2004) 235–244.
- [49] S. Laforge, D. Martin, J.L. Paillaud, M. Guisnet, *J. Catal.* 220 (2003) 92–103.
- [50] D. Meloni, D. Martin, M. Guisnet, *Appl. Catal. A: Gen.* 215 (2001) 67–79.
- [51] M. Guisnet, L. Coste, F. Ramoa Ribeiro, *J. Mol. Catal. A: Chem.* 305 (2009) 69–83.
- [52] P. Matias, J.M. Lopes, S. Laforge, P. Magnoux, P.A. Russo, M.M.L. Ribeiro Carrot, M. Guisnet, F. Ramoa Ribeiro, *J. Catal.* 259 (2008) 190–202.
- [53] D.M. Bibby, N.B. Milestone, J.E. Petterson, L.A. Aldridge, *J. Catal.* 97 (1986) 493–502.
- [54] A.R. Pradhan, J.F. Wu, S.J. Jong, T.C. Tsai, S.B. Liu, *Appl. Catal. A: Gen.* 165 (1997) 489–497.